Amino Acids (2011) 41:387–399
DOI 10.1007/s00726-010-0668-2

ORIGINAL ARTICLE

SILAC-based proteomic analysis to dissect the "histone modification signature" of human breast cancer cells

Alessandro Cuomo · Simona Moretti · Saverio Minucci · Tiziana Bonaldi

Received: 19 March 2010 / Accepted: 16 June 2010 / Published online: 9 July 2010

Abstract In living cells, the N-terminal tails of core histones, the proteinaceous component of nucleosomes, are subjected to a range of covalent post-translational modifications (PTMs), which have specific roles in modulating chromatin structure and function. A growing body of evidence suggests that deregulation of histone modification patterns, upstream or downstream of DNA methylation, is a critical event in cancer initiation and progression. However, a comprehensive description of how histone modifications, singly or in combination, is disrupted in transformed cells is missing; consequently the issue whether and how specific changes in histone PTMs patterns correlate to particular tumor features is still elusive. In the present study, we focused on human breast cancer and comprehensively analyzed PTMs on histone H3 and H4 from four cancer cell lines (MCF7, MDA-MB231, MDA-MB453 and T-47D), in comparison with normal epithelial breast cells. We performed high-resolution mass spectrometry analysis of histones, in combination with stable isotope labeling with amino acids in cell culture (SILAC), to quantitatively track the modification changes in cancer cells, as compared to their normal counterpart. Our investigation focuses on lysine acetylation and methylation on fourteen distinct sites in H3 and H4. We observed significant changes for several modifications in cancer cells: while in a few cases those modifications had been previously described as a hallmark of human tumors, we could identify novel modifications, whose abundance is significantly altered in breast cancer cells. Overall, these modifications may represent part of a "breast cancer-specific epigenetic signature", with implications in the characterization of histone-related biomarkers. This work demonstrates that SILAC-based proteomics is a powerful tool to study qualitatively and quantitatively histone PTMs patterns, contributing significantly to the comprehension of epigenetic phenomena in cancer biology.

Keywords Mass spectrometry · Quantitative proteomics · Epigenetic mark · Histones · Breast cancer

Abbreviations

MS	Mass spectrometry
LC-MS/MS	Liquid chromatography coupled to tandem mass spectrometry
SILAC	Stable isotope labeling with amino acid in cell culture
hPTMs	Histone post-translational modifications
HDACs	Histone deacetylases
HMTs	Histone methyl-transferases
FA	Formic acid
ACN	Acetonitrile
Ac	Acetylation
me1	Mono-methylation
me2	Di-methylation
me3	Tri-methylation

A. Cuomo and S. Moretti contributed equally to this work.

Electronic supplementary material The online version of this article (doi:10.1007/s00726-010-0668-2) contains supplementary material, which is available to authorized users.

A. Cuomo · S. Moretti · S. Minucci · T. Bonaldi (✉)
Department of Experimental Oncology,
European Institute of Oncology (IEO),
IFOM-IEO Campus, Via Adamello 16, 20139 Milan, Italy
e-mail: tiziana.bonaldi@ifom-ieo-campus.it

S. Minucci
Department of Biomolecular Sciences and Biotechnology,
University of Milan, via Celoria 26, 20133 Milan, Italy

Introduction

Post-translational modifications (PTMs), such as phosphorylation, acetylation, methylation, and ubiquitination are key regulatory elements of proteins function during development, growth and differentiation. The four core histones, around which the DNA is wrapped within the chromatin, are prototype of multi-site modified proteins, being susceptible to a variety of PTMs (Kouzarides 2007). The combinatorial pattern of these modifications defines an epigenetic code, marking different functional regions on chromatin (Dobosy and Selker 2001; Jenuwein and Allis 2001).

It is becoming widely accepted that perturbations of this "molecular bar code" can play a pivotal role in the onset, progression and maintenance of cancer. The field of cancer epigenetics focused initially on aberrant DNA methylation (Feinberg and Vogelstein 1983; Esteller 2002; Herman and Baylin 2003). However, it is now apparent that changes in methylation of genomic DNA occur in the context of a more composite epigenetic deregulation, involving histone PTMs (hPTMs). Distinct alterations in the pattern of hPTMs have been identified in cancer cells, with clinical relevance in a few cases (Fraga et al. 2005; Seligson et al. 2005). Along the same line of evidence, immunohistochemistry analysis of hPTMs in human breast cancer revealed that loss of DNA methylation is accompanied by a global reduction of H4K16 acetylation (Elsheikh et al. 2009). In addition, moderate to complete reduction of lysine acetylation (H3K9, H3K18 and H3K12) and methylation (H3K9me3, H4K20me3) was observed during malignant breast cancer progression (Tryndyak et al. 2006; Kovalchuk et al. 2007; Elsheikh et al. 2009; Suzuki et al. 2009). Furthermore, altered histone modification patterns correlate with different tumor subtypes and may function as prognostic factors, with important applications in clinical research (Elsheikh et al. 2009). In spite of the strong interest and the recent efforts in profiling its epigenome, the global portrait of breast cancer-specific hPTMs signature is still incomplete.

Antibodies specifically raised against different modifications are commonly employed to study the code of hPTMs (Pokholok et al. 2005). Although advantageous for their sensitivity and the standardized protocols, antibody-based assays are hampered by limitations regarding specificity, detection of adjacent modifications and linearity of signal (Garcia et al. 2007). Mass spectrometry (MS) has already proved to be an efficient alternative to map complex patterns of PTMs on histones, overcoming the limitations faced with antibodies (Beck 2010). Furthermore, high-resolution mass spectrometers, such as the Fourier-transform ion cyclotron resonance (FT-ICR) mass analyzer or the new generation Orbitrap, offer a significant improvement to the MS-analysis of hPTMs, because these instruments can resolve efficiently nearly isobaric modifications, such as acetylation (42.011 Da) and tri-methylation (42.047 Da), even on very long polypeptides (for instance spanning the entire N-terminal tails of the core histones), up to intact proteins (Jung et al. 2010). The MS strategy where intact proteins are ionized and then introduced to a mass analyzer is called "top-down" approach (Kelleher et al. 1999). This analytical strategy, with the associated concept of "Shotgun Proteins Annotation" (Pesavento et al. 2004) were initially applied to the analysis of alternative splicing events in proteins (Roth et al. 2005) and then have been extended to the in depth-characterization of proteins variants and post-translationally modified species. Top-down MS has been successfully applied to study histones micro-heterogeneity (Freitas et al. 2004; Burlingame et al. 2005), generating comprehensive maps of hPTMs, with the advantage of informing about the overall abundance of differentially modified protein species and about the relative stoichiometry of PTMs combination within an intact protein (Medzihradszky et al. 2004; Thomas et al. 2006; Garcia et al. 2007). More recently, a development of top-down, named "middle-down" MS, has been introduced to analyze large protein fragments (>3 kDa), potentially matching with protein sub-domains and deriving from the enzymatic digestion with proteases that cleave less frequently than trypsin, thus releasing larger peptides. Middle-down combines benefits of both peptide-based analysis (bottom-up) and top-down approach (Taverna et al. 2007).

To further characterize hPTMs in human tumors and to shed light on the relationship between epigenetic marks and cancer features, we undertook a proteomic approach to profile hPTMs changes in a representative panel of breast cancer cell lines (MCF7, MDA-MB231, MDA-MB453 and T-47D), compared with normal epithelial breast cells (MCF10A). To quantitatively compare hPTMs profiles, we employed stable isotope labeling with amino acids in cell culture (SILAC) strategy, consisting of labeling cells through normal metabolic processes by incorporation, upon division, stable isotope-coded amino acids in newly synthesized proteins (Ong et al. 2004) SILAC media are prepared where natural amino acids are replaced by isotope-coded 'light" (L) and "heavy" (H) amino acids. Cells grown in these media incorporate the light or heavy amino acids, with no effect on cell physiology. When L and H cell populations are mixed, their proteins and peptides remain distinguishable by MS; protein abundances is calculated based on the relative MS signal intensities of the corresponding peptides. SILAC provides accurate relative quantification and enables development of elegant functional assays in proteomics (Mann 2006). Here, we describe the extension of SILAC method to the

quantification of modified peptides from histones H3 and H4: metabolic labeling was achieved with heavy-arginine only and quantification carried out at the peptide level, calculating the ratio of modified peptides between cancer and normal histones.

We profiled 24 distinct modifications at 14 different sites of the N-terminal tails of histone H3 and H4, covering histone marks that are functionally well-characterized. Our results demonstrate the possibility of defining a specific "breast cancer histone modification signature" that includes not only already described hallmarks of human tumors, but also novel modifications previously not described in tumors. These findings extend our knowledge of hPTMs patterns in breast carcinoma, with a detailed epigenetic phenotypization of breast cancer subtypes.

Materials and methods

Stable isotope labeling of histones in normal and tumor breast epithelial cell

Normal MCF10A epithelial breast cells and MCF7, MDA-MB231, MDA-MB453 and T-47D breast cancer cells were obtained from the American Type Culture Collection (ATCC, Manassas, VA, USA). MCF10A cells were grown in lysine- and arginine-free DMEM/Ham's F12 (1:1), supplemented with 5% dialyzed fetal bovine serum (FBS) (Invitrogen 26400-044), 2 mM L-glutamine, 20 ng/ml human epidermal growth factor (EGF), 50 ng/ml cholera toxin, 10 ng/ml human insulin, 0.5 μg/ml human transferrin. Light isotope-coded lysine and arginine (Lys0 and Arg0) were added at a concentration of 146 and 84 mg/l, respectively. For the "heavy" labeling of the four breast cancer cell lines, DMEM (Invitrogen) depleted of lysine and arginine was supplemented with 10% dialyzed FBS, 100 units/ml penicillin/streptomycin (Invitrogen), 2 mM Glutamax (Invitrogen), 146 mg/l of light lysine (Lys0) and 84 mg/l of heavy arginine ($^{13}C_6^{15}N_4$L-Arginine, Arg10, Sigma, 608033). Cells were maintained at 37°C in a humidified incubator with 5% CO_2–95% air atmosphere and diluted every 3 days. Growth in SILAC media was carried out until reaching at least six replications, to ensure complete histone labeling.

Purification and enzymatic digestion of histones

For each of the four SILAC heavy/light experiments, light-labeled MCF10A cells were mixed in equal amount with the four distinct types of heavy-labeled breast cancer cell lines, to reach a total of 20×10^6 cells. The (1:1) cell mixture was homogenized in lysis buffer [10% Sucrose, 0.5 mM EGTA pH 8.0, 15 mM NaCl, 60 mM KCl, 15 mM HEPES, 0.5% Triton, 0.5 mM PMSF, 1 mM DTT, 5 mM NaF, 5 mM Na_3VO_4, 5 mM NaButyrate, cocktail of protease inhibitors (Sigma)]; nuclei were separated from cytoplasm by centrifugation on sucrose cushions, washed twice in cold PBS and then extracted in 0.4 N HCl for an overnight, at 4°C. Core histones, soluble in supernatants together with linker histones and high mobility group (HMG) proteins, were dialyzed against 100 mM ice-cold CH3COOH, using dialysis tubing with 6–8 kDa cutoff. The dialyzed samples were lyophilized and stored at −20°C.

Yield and purity of histone fractions were evaluated by Bradford assay and SDS–PAGE, respectively. Approximately, 8 μg of core histones were digested in solution with endoproteinase Arginine-C (Arg-C; Roche) according to the manufacturer's protocol, at 37°C, for an overnight. Digested peptides were desalted and concentrated using a combination of reverse-phase C18/Carbon and ion-exchange (SCX) chromatography on hand-made nano-columns (StageTips) (Rappsilber et al. 2007): samples loaded on C18/Carbon and SCX StageTips where eluted with high organic solvent (80% ACN) and NH4, respectively. Eluted peptides were lyophilized, re-suspended in 0.1% FA and 5% ACN in ddH2O, pooled and subjected to LC–MS/MS analysis.

Liquid chromatography and tandem mass spectrometry

Peptide mixtures separated by nano-liquid chromatography using an Agilent 1100 Series nanoflow LC system (Agilent Technologies), directly interfaced to a LTQ-FT Ultra mass spectrometer (ThermoFisher Scientific, Bremen, Germany). The nanoliter flow LC was operated in one column set-up with a 15 cm analytical column (75 μm inner diameter, 350 μm outer diameter) packed with C18 resin (ReproSil, Pur C18AQ 3 μm, Dr. Maisch, Germany). Solvent A was 0.1% FA and 5% ACN in ddH2O and solvent B was 95% ACN with 0.1% FA. Samples were injected in an aqueous 0.1% TFA solution at a flow rate of 500 nl/min. Peptides were separated with a gradient of 0–40% solvent B over 90 min followed by a gradient of 40–60% for 10 min and 60–80% over 5 min at a flow rate of 250 nl/min. The nanoelectrospray ion source (Proxeon, Odense, Denmark) was used with a spray voltage of 1.5–2.0 kV. No sheath, sweep and auxiliary gasses were used and capillary temperature was set to 180°C. The mass spectrometer was operated in a data-dependent mode to automatically switch between MS and MS/MS acquisition. In the LTQ-FT Ultra, full scan MS spectra were acquired at a target value of 2,000,000 ions and with a resolution of 100,000 (FWHM) at 400 m/z. In the LTQ MS/MS, spectra were acquired using a target value of 5,000 ions and the five most intense ions were isolated for CID-fragmentation with a normalized

collision energy setting of 35. The dynamic exclusion time was set to 90 s. Each sample was analyzed in three technical replicates.

Analysis of mass spectrometric data and quantitation of SILAC-labeled peptides

The raw data from LTQ-FT Ultra were converted to mgf files using Raw2MSM software (Olsen JV, 2005). MS/MS spectra were first searched by Mascot Daemon (version 2.2.2, Matrix Science) against the IPI_human database (version 6.63) (containing 76539 sequences; 31960612 residues). MS mass tolerance was set to 7 ppm and MS/MS mass tolerance was set to 0.8 Da. Variable modifications included mono- and di-methylation on lysine and arginine residues, tri-methylation, acetylation on lysines, oxidation on methionine and acetylation on N-terminal of proteins. In addition, heavy isotope-labeled peptides with PTMs were identified by Mascot search by including Arginine-$^{13}C_6^{15}N_4$ (Arg10) as variable modification. Peptides containing modifications were manually quantified using the Qual-Browser version 2.0.7 (ThermoFisher Scientific). Extracted ion chromatograms were constructed for each precursor *m/z* value with mass tolerance 10 ppm and mass precision up to four decimal places. Peak areas for each pair of heavy and light peptides were measured within the same retention time interval. The SILAC ratio was calculated between the peak areas of pairs of light and heavy peptides for H3 and H4.

The same raw data were also further analyzed by MaxQuant software, version 1.0.13.13 (Cox and Mann 2008). Mascot searching parameters were as above, but the IPI_human database used was combined with a list of 175 common contaminants, and concatenated with the reversed versions of all sequences (so-called "Decoy database", Kall et al. 2008). Arg10 was specified as labeled amino acid; maximally three missed cleavages and three labeled amino acids per peptide were allowed. MaxQuant is suited for high-resolution mass spectrometry data and automatically detects peaks, isotope clusters and SILAC-labeled peptide pairs as 3D objects in m/z, taking in account elution time and signal intensity. The false discovery rate for peptides was set to 0.01, with a minimum length of 6 amino acids. In addition, a posterior error probability for each MS/MS spectrum was set to be at most 0.1. In order to correct for potential error in mixing of light and heavy cells that could generate errors in quantification of modified SILAC-paired peptides, we calculated a "correction factor" (CF), measured as the average of the relative heavy and light intensities (SILAC ratio) for the monoisotopic peaks from three different unmodified peptides for both H3 and H4 (Table S1). The mean of the CF is 1.12 with standard deviation (STDEV) 0.13. All ratios for the modified peptides from each of the four independent SILAC experiments were corrected for the corresponding CF. Furthermore, the 1 ± SD value for each CF was used to define the experimental range of variation of the ratio measurement, used as "cutoff" to discriminate significant changes in PTMs from noise (STDEV is represented by a red-dotted line in Fig. 3).

Western blot analysis of histone modifications and protein expression

Breast cancer cell extracts were prepared dissolving about 5×10^6 cells in 500 µl of lysis buffer (10 mM Tris–HCl, pH 8.0; 1% Triton; 0.1% SDS; 0.1% sodium deoxycholate; 140 mM NaCl; 1 mM EDTA; 1 mM PMSF; 1 mM DTT; cocktail of protease inhibitors at concentration 1 µg/ml; 1 mM Na_3VO_4, 1 mM NaF, and 1 mM NaButyrate). Lysates were sonicated, incubated at 4°C for 30 min and then centrifuged at 13,000 rpm at 4°C for 15 min. Equal amounts of protein extracts were separated in 10–17% SDS–PAGE and transferred to nitrocellulose membranes. Membranes were incubated at 4°C overnight with primary antibodies specific for the following modifications and enzymes: H3K9me2 (Abcam 1220), H3K4me1 (Abcam 8895), H3K27me3 (Upstate Millipore 07-449); H4K5ac (Upstate Millipore 06-759); unmodified histone H3 (Abcam 1791); G9a (Abcam 31874); Suv39H1 and Suv39H2 (Abcam 38637 and 71683, respectively); SET-DB1 (Abcam 5430); EZH2 (Abcam 3748); Pr-SET7 (Abcam 3798); HDAC1, HDAC2 and HDAC3 (Abcam 7028, 7029 and 7030, respectively). Antibody binding was revealed by ECL Plus® Immunoblotting Detection System (Amersham Biosciences). Images are representative of three independent immunoblots; antibody anti-unmodified H3 was used as loading control.

Results

MS-based comparative analysis of histone PTMs in breast cancer cells

To label normal and cancer cells with isotope-coded amino acids, they were grown in SILAC media for six generations. Careful monitoring of growth rate, viability and overall morphology for approximately two weeks demonstrated no alteration from physiology, compared to cells cultured in standard medium. After six cell doublings Arg10 incorporation reached about 97%; prolonged culturing in SILAC medium did not result in significant overall increase of incorporation in histones (data not shown). Hence six replications were fixed as our standard labeling time.

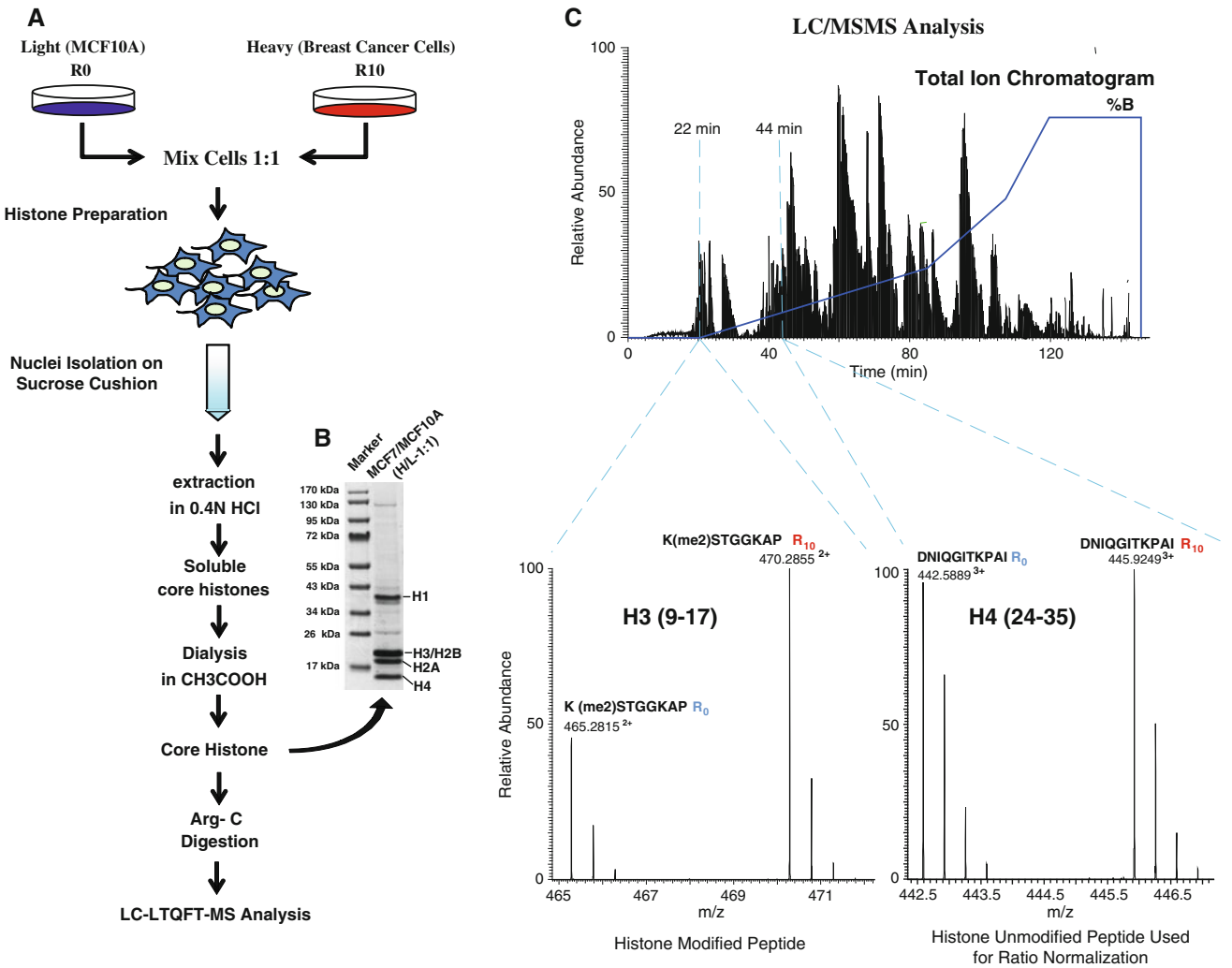

Fig. 1 Schematic representation of SILAC approach combined to high resolution-MS analysis for the precise quantitation of histone PTMs in breast cancer cell lines. **a** MCF10A and tumor cells were grown in light (Arg0) and heavy (Arg10) SILAC medium, respectively. After six generations, cells were harvested and mixed in equal amount (1:1). Nuclei were separated from extracts by centrifugation on 10% sucrose cushions. Core histones were extracted in 0.4 M HCl, dialyzed against ice-cold acetic acid and in-solution digested with Arg-C. Peptides mixtures were subjected to nano-LC-MS/MS analysis. **b** Five micrograms of histones were loaded on 4–12% SDS–PAGE. Histone H3, H4, H2A and H2B are visible around the 17-kDa marker band; H3 and H2B co-migrate in the same band. (**c**, *upper panel*) Total Ion Chromatogram relative to the Arg-C digestion of core histones purified from MCF7 (H)/MCF10 (L): peptides are separated with a stepwise gradient of ACN in 120 min (*smooth line* denoting chromatogram) (**c**, *lower left panel*). SILAC pair at m/z 465.2815 and 470.2855 corresponds to the di-metylated peptides H3 (9–17), with ratio 1.4. **c**, *lower right panel* H4 (24–35), is one of the unmodified peptides used for CF calculation, as described in "Analysis of mass spectrometric data and quantitation of SILAC-labeled peptides"

Each of the four breast cancer cell lines, grown in "heavy" medium, was independently mixed in equal amounts (1:1) with normal MCF10A epithelial breast cells, cultured in "light" medium. Histones were extracted from nuclei with a well-established protocol that allows their efficient and fast enrichment in strong-acidic conditions, as described in Fig. 1a; yield and purity of the preparation was evaluated in 4–12% SDS–PAGE gradient gels (Fig. 1b): core histones were enriched from background, together with linker histone H1 and HMG proteins. Each H/L histone preparation was then digested with endoproteinase Arg-C that cleaves at the amide bond C-terminal to arginine residue, producing peptides with an optimal length for MS analysis and which, on average, contain a limited number of lysines in vivo modified. Protease digestion in solution increases the peptide recovery and, consequently, the sequence coverage. Digested peptides were analyzed by LC–MS/MS on a LTQ-FT Ultra mass spectrometer. Figure 1c exemplifies the strategy followed for relative quantification of modified peptides. The upper panel represents the total ion chromatogram (TIC) relative to Arg-C digested histones from MCF7/MCF10 (H/L) cells, separated by nano-RPLC and detected by MS (Fig. 1c, upper panel). The mass spectrum of peptides eluting at 22.02 min

shows a pair of heavy and light peptides of value 465.2815 and 470.2855 m/z, assigned by MS/MS analysis to the di-methylated peptide (9–17) of histone H3 (Fig. 1c, lower left panel). The two peptides within the SILAC pair share the amino acidic sequence (KSTGGKAPR), but they differ in mass due to the incorporation of the different isotope-coded arginines. The relative intensity of the H and L peaks is proportional to the relative abundance of the corresponding peptides from the two samples; modified peptide ratios were corrected using the CF, to adjust for potential mixing errors, as described in "Materials and methods" (Fig. 1c, lower right panel).

Our comprehensive MS analysis focused on histones H3 and H4 and allowed site-specific identification of 24 distinct PTMs. Representative MS/MS spectra for modified peptides in the cell lines analyzed are reported in supplementary Fig. S2. With the aim of gaining a bird-eye view on the relative stoichiometry of all modifications, we calculated a "global peptide species percentage" (GP) for each modified histone peptide from the five different cell types (Pesavento et al. 2004; Jung et al. 2010). The GP value represents the relative proportion of each modified species among all quantified sub-species with the same amino acid sequence. The bar chart in Fig. 2 shows GP (%) values, calculated for all modified histone peptides from MCF10A cells. GP analysis indicates that H3K9me2/K14ac (42%), H3K27me2/K36me2 (62%) and H4K20me2 (90%) are predominant modifications in MCF10A cells. Surprisingly, other modifications were very poorly represented (such as H3K4me1, me2 and me3, see below). Using these cells as a reference, we then extended the GP analysis to the four breast cancer cell lines and the results are summarized in Table 1.

Profiling PTMs on histone H3 between normal and breast cancer cells

Initially, our analysis focused on studying the PTMs patterns of histone H3. Among the four core histones, H3 contains the largest number of modifications, annotated and functionally characterized. In mammals, H3 is present in three variants: H3.1, H3.2, and H3.3 (plus a testis-specific H3.1t of unknown function). Variants H3.1 and H3.2 differ of only a single amino-acid substitution at residue 96, where a Cysteine in H3.1 is replaced by a Serine in H3.2. Variant H3.1 is exclusively expressed during S phase, coordinately with the other core-histones and it is assembled into nucleosomes in a replication-dependent manner (Loyola et al. 2006). H3.1/2 differs from H3.3 for amino acid substitutions at positions 31, 87, 89, 90, and 96. Variant H3.3 is expressed throughout the cell cycle, although at much lower rate, and its assembly into

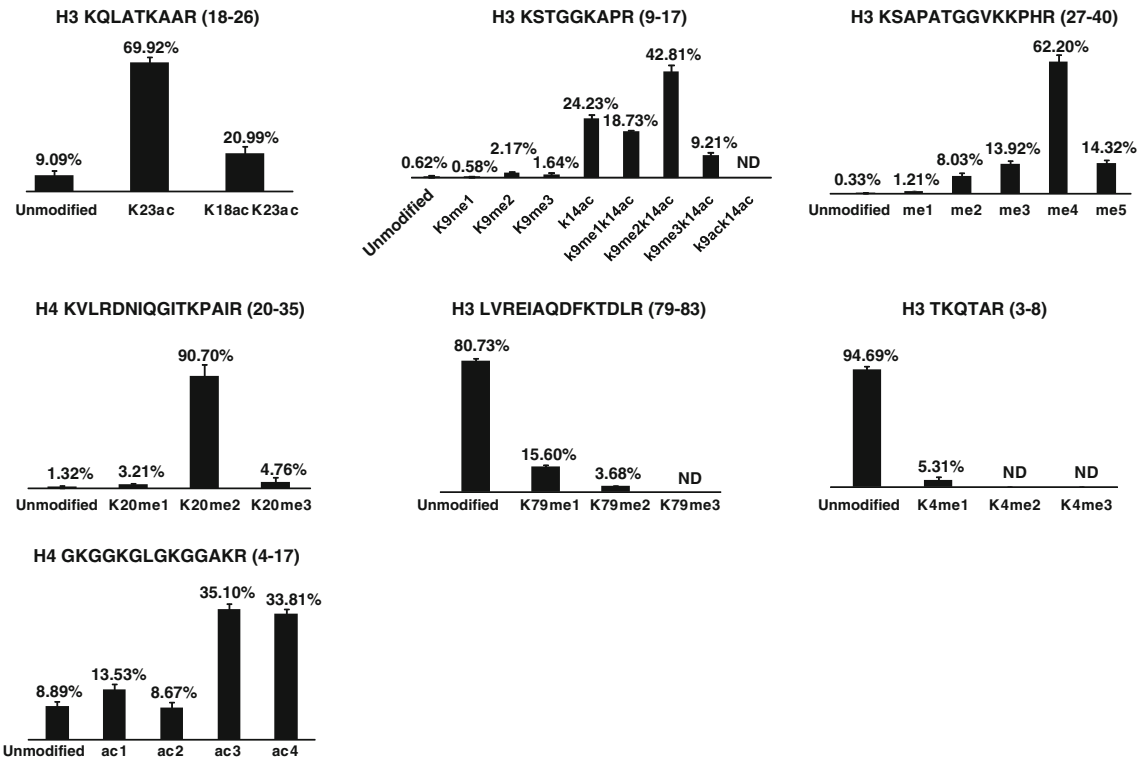

Fig. 2 Global species percentage (GP) profile of H3 and H4 peptides from MCF10A cells H3K9me2/K14ac (42%), H3K27me2/K36me2 (62%) and H4K20me2 (90%) are predominant modifications in MCF10A cells lines

Table 1 Global peptide species percentage (GP) analysis in MCF10A and breast cancer cells

PTMs	MCF10A (±SD)	MCF7 (±SD)	MB-231 (±SD)	MB-453 (±SD)	T-47D (±SD)
H3 TKQTAR (3–8)					
Unmodified	94.69% ± 0.02	87.87% ± 0.01	85.53% ± 0.09	87.71% ± 0.11	89.87% ± 0.05
K4me1	5.31% ± 0.02	12.13% ± 0.01	14.47% ± 0.09	12.29% ± 0.10	10.13% ± 0.07
K4me2	nd	nd	nd	nd	nd
K4me3	nd	nd	nd	nd	nd
H3 KSTGGKAPR (9–17)					
Unmodified	0.62% ± 0.32	0.76% ± 0.07	0.84% ± 0.49	0.13% ± 0.11	0.25% ± 0.19
K9me1	0.58% ± 0.26	0.46% ± 0.15	0.86% ± 0.39	0.10% ± 0.05	0.21% ± 0.16
K9me2	2.17% ± 0.48	3.34% ± 0.41	12.50% ± 4.1	1.35% ± 0.92	2.53% ± 0.67
K9me3	1.64% ± 0.57	0.50% ± 0.03	2.13% ± 0.64	0.13% ± 0.11	0.28% ± 0.25
k14ac	24.23% ± 1.44	24.56% ± 4.25	12.42% ± 1.35	14.31% ± 1.90	20.81% ± 2.58
k9me1k14ac	18.73% ± 0.65	17.78% ± 0.82	10.80% ± 1.60	16.05% ± 0.02	16.30% ± 1.23
k9me2k14ac	42.81% ± 2.67	42.91% ± 4.05	43.10% ± 5.54	56.48% ± 1.98	47.42% ± 5.91
k9me3k14ac	9.21% ± 0.93	9.69% ± 0.16	17.35% ± 0.12	11.44% ± 1.15	12.20% ± 0.82
k9ack14ac	nd	nd	nd	nd	nd
H3 KQLATKAAR (18–23)					
Unmodified	9.09% ± 2.16	11.98% ± 0.05	6.03% ± 1.88	8.41% ± 4.63	7.27% ± 2.98
K23ac	69.92% ± 2.75	80.39% ± 1.67	66.06% ± 6.72	66.95% ± 5.66	72.36% ± 9.73
K18acK23ac	20.99% ± 3.6	7.63% ± 1.6	27.91% ± 8.60	24.64% ± 1.02	20.36% ± 12.71
H3.1/2 KSAPATGGVKKPHR (27–40)					
Unmodified	0.33% ± 0.19	0.20% ± 0.08	0.30% ± 0.29	0.06% ± 0.08	0.50% ± 0.18
me1	1.21% ± 0.43	1.23% ± 0.50	0.73% ± 0.20	0.34% ± 0.10	1.12% ± 0.08
me2	8.03% ± 1.80	15.18 ± 3.82	13.62% ± 0.22	8.58% ± 0.49	11.20% ± 1.18
me3	13.92% ± 1.47	21.77% ± 2.59	19.96% ± 2.4	17.93% ± 0.52	17.31% ± 2.10
me4	62.20% ± 3.14	52.06% ± 7.16	56.58% ± 4.10	63.48% ± 2.17	59.68% ± 3.64
me5	14.32% ± 1.31	9.56% ± 0.16	8.81% ± 1.76	9.62% ± 1.34	10.18% ± 0.02
H3 EIAQDFKTDLR (73–83)					
Unmodified	80.73% ± 1.27	82.87% ± 1.06	84.06% ± 0.40	84.84% ± 0.01	82.84% ± 0.36
K79me1	15.60% ± 1.08	13.62% ± 0.80	13.48% ± 0.63	12.51% ± 0.05	14.97% ± 0.53
K79me2	3.68% ± 0.27	3.51% ± 0.26	2.46% ± 0.23	2.65% ± 0.03	2.19% ± 0.16
K79me3	nd	nd	nd	nd	nd
H4 GKGGKGLGKGGAKR (4–17)					
Unmodified	8.89% ± 3.92	10.31% ± 1.49	3.87% ± 0.07	5.20% ± 0.58	4.82% ± 4.8
ac1	13.53% ± 3.86	27.58% ± 3.46	6.98% ± 1.40	6.62% ± 0.86	11.36% ± 7.50
ac2	8.67% ± 3.90	14.28% ± 3.81	7.59% ± 7.68	4.81% ± 1.71	13.71% ± 17.1
ac3	35.10% ± 6.29	27.43% ± 1.61	43.91% ± 5.77	44.96% ± 1.02	33.81% ± 15.7%
ac4	33.81% ± 3.22	20.39% ± 4.11	37.65% ± 3.31	38.42% ± 0.74	36.30% ± 13.7
H4 KVLRDNIQGITKPAIR (20–35)					
Unmodified	1.32% ± 0.60	5.08% ± 0.22	7.54% ± 0.21	5.48% ± 1.65	5.13% ± 0.27
K20me1	3.21% ± 0.60	5.10% ± 0.36	16.17% ± 0.78	6.35% ± 1.55	5.77% ± 0.35
K20me2	90.70% ± 0.83	86.88% ± 0.34	75.89% ± 0.73	85.07% ± 3.31	86.67% ± 0.74
K20me3	4.76% ± 0.67	2.94% ± 0.18	0.40% ± 0.16	3.10% ± 0.10	2.43% ± 0.12

chromatin is replication-independent, with a preference for active regions, where chromatin is more fluid and dynamic due to remodeling associated with transcription (Thomas et al. 2006). Thanks to these differences in the primary sequence, H3 variants can be separated via reversed-phase HPLC and different protocols have been established. This opportunity allows the independent MS analysis of the separated variants, with improved assignment of PTMs patterns to each distinct peptide spices, both by bottom-up or top-down strategies (Cosgrove 2007; Su et al. 2007).

In our study, instead, we carried out LC–MS/MS analysis of preparations of total histone octamers, in solution digested with Arg-C without a preceding HPLC separation. Our aim was in fact to create a straightforward method to identify and quantify hPTMs in a single analysis, reducing the sample manipulation and the amount of starting material. As such, we omitted the RP-LC step to separate the histones variants and thus we could not attribute unambiguously to distinct H3 subtypes the peptides sharing the amino acid sequence. Hence, here we assign generically to "H3" all the characterized peptides whose sequence is undistinguishable between the variants. Instead, peptide (27–40) is distinguishable between H3.1/2 and H3.3, thanks to the substitution of Alanine 31 (KSAPATGGVKKPHR) with Serine (KSAPSTGGVKKPHR); in this case we can assign a specific nomenclature. We could also identify the peptide (84–116), specific for H3.1/2 (Fig. S2), but this fragment does not bear PTMs.

Peptide (9–17) contains two lysines, K9 and K14, which are both subjected to post-translational modifications: while K9 was found mono-, di- and tri-methylated, K14 was preferentially found acetylated (Fig. 3); different levels of K9 methylation co-exist with K14 either unmodified or acetylated (Fig. S1). Although K9 acetylation was already reported in breast carcinoma tissues (Elsheikh et al. 2009), this modification was not detected in our analysis, probably due to its low abundance in these cells.

We observed loss of K9me3 and a parallel increase of K9me2 in tumor versus normal cells; change in di-methylated K9 has not been previously described and it was confirmed by Western blot analysis (Fig. 4). A slight decrease of K14ac was observed in MDA-MB231 and MDA-MB453 cells, but not in MCF7 and T-47D cells. Moreover, we observed that di- and tri-methylation of K9 change significantly on peptides not containing K14 acetylated, while the methylation changes are not significant in the case of K9me(x)/K14ac (Fig. S1). This observation suggests that only specific chromatin regions characterized by K9 methylation and absence of K14 acetylation, representing only a minor fraction of chromatin, are affected in cancer cells.

Peptide (18–26) was identified as mono- and di-acetylated on K23 and K18, respectively. The peptide containing K18ac/K23ac is less abundant only in MCF7 compared to MCF10A, while the other tumor lines did not vary significantly (Fig. S1).

Peptide (27–40) from variants H3.1/2 (KSAPATG GVKKPHR) contains three lysine residues, K27, K36 and K37, which are subjected to enzymatic methylation in vivo.

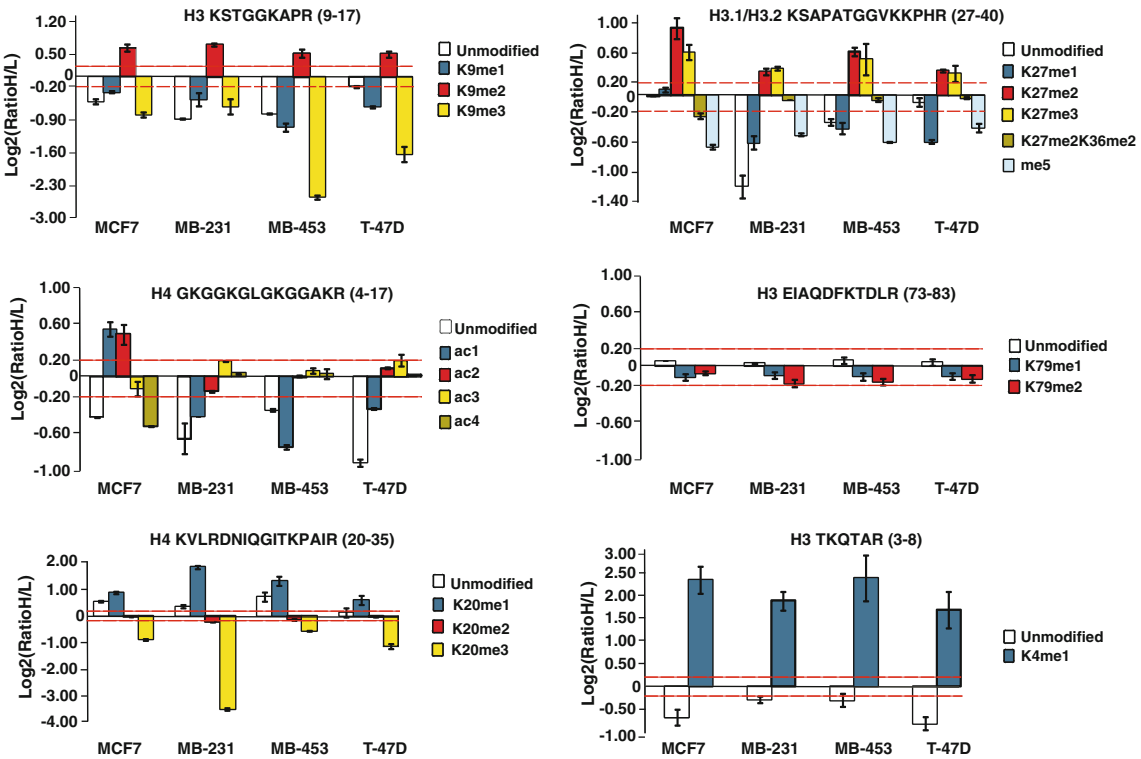

Fig. 3 Relative quantification of histone modifications in breast cancer cells versus non-tumor breast cells SILAC ratios in $\log_2$ scale for histone H3 and H4 peptides. *Horizontal dashed line* defines the $1 \pm$ SD calculated for the ratios of non-modified peptides from a total of twelve LC runs, as described in "Analysis of mass spectrometric data and quantitation of SILAC-labeled peptides"

We detected this peptide in several distinct modified species, from mono- to penta-methylated (me1 to me5): K27 residue was identified as mono-, di-, and tri-methylated (MS/MS fragmentation spectra relative to this modification are reported in Fig. S2); K27me2 was also found in association with K36me2, within the me4 peptide (Fig. 3, S2). The fragmentation of me5 peptide produced highly complex spectra, due to the large number of isobaric modified species eluting within a very short time-window during the nano-LC. We could not uniquely assign all possible modification sites for the me5; however, we identified two of the most probable species employing the best 'localization probability score' as calculated by Mascot software (Olsen et al., 2005): K27me3/K36me2 and K27me3/K36me1/K37me1 (Fig. S2). The quantitative analysis of changes in methylation profiles of this peptide showed that K27me2 and K27me3 increase in breast cancer (Fig. 3); Western blot analysis with an antibody specific for H3K27me3 confirmed this result (Fig. 4). In addition, we observed a down-regulation of the penta-methylated peptide in breast cancer, which could be due to a reduction of both K36me1 and K37me1, given the observed increase of K27me3.

The complete pattern of methylation (me1–me5) for the peptide (27–40) from variant H3.3 (KSAPSGGV KKPHR) was difficult to detect without preceding RP-LC separation. In fact, we observed a significant overlap with the modified species of peptide (27–40) from H3.1/2, eluting together within a short time range (27.07–27.40 min) in LC gradient. Furthermore, due to the higher abundance of H3.1/2 variants, the signals of the corresponding peptides were dominating the full-MS spectra, masking H3.3 ones (Fig. S3a). However, even in this condition, we could observe a delayed elution of the tetra-methylated species from both variants, which allow to resolve the H3.3 (27–40) me4 specie over co-eluting peaks from H3.1/2, and thus to uniquely identify its modification status (Fig. S3b). Upon MS/MS we could site-specific attribute the four methylation to K27me2, in association with K37me2 (Fig. S2). However, the comparative analysis of this mark among the five cell lines under study did not reveal significant changes in abundance between normal and cancer types (Fig. S3).

Peptide (3–8) was identified as unmodified and mono-methylated (Fig. 3) and the SILAC measurement indicated a significant decrease of K4me1 in tumor cells; this is an entirely novel observation and it was further validated by Western blot analysis (Fig. 4). As observed in MCF10A cells, di- and tri-methylated forms of K4 were detected neither in MS nor Western blot analysis: presumably their abundance in vivo in these cell types is below the detection limit of both analytical approaches.

Peptide (73–83) was identified as mono-, di-, and tri-methylated on Lysine 79. The abundance of this mark did not significantly change in cancer compared to normal cells (Fig. 3).

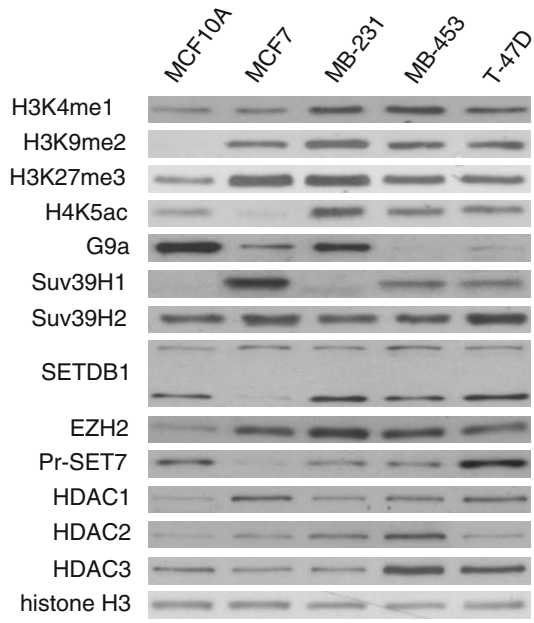

Fig. 4 Western blot analysis of hPTMs, and of HMTs and HDACs expression in human breast cancer cells. Cell extracts from MFC10A, MCF7, MDA-MB231, MDA-MB453 and T-47D were subjected to immunoblotting using primary antibodies against H3K4me1, H3K9me2, H3K27me3 and H4K5ac, as described in "Western blot analysis of histone modifications and protein expression". Expression levels of the enzymes G9a, Suv39H1, Suv39H2, SETDB1, EZH2, Pr-SET7, HDAC 1, 2 and 3 are also shown. The antibody anti-SETDB1 detects two bands of 170 and 143 kDa (the predicted molecular weight) as reported in the data sheet. Unmodified histone H3 is the loading control. Blots are representative of three independent experiments

Profiling PTMs on Histone H4 between normal and breast cancer cells

The complex acetylation pattern of the N-terminal tail of histone H4 revealed by quantitative MS-analysis is schematized in Fig. 3 (bottom left panel). The peptide (4–17) is present in several modified species, from mono- to tetra-acetylated ones. The four possible acetylations are distributed over K5, K8, K12, and K16 residues, with the following localization probability, suggested by the analysis of fragmentation data: K16 is the prevalent sites for mono-acetylation, and K16/K12, K16/K12/K8 and K16/K12/K8/K5 for di-, tri- and tetra-acetylation, respectively. This is in accordance with the 'zip model' that suggests that acetylation propagates from K16 to K5 of H4 and that, consequently, simultaneous acetylation at K5 and K8 indicates hyper-acetylated H4 (Thorne et al. 1990; Zhang et al. 2002) (Fig. S2).

In MDA-MB231, MDA-MB453 and T-47D cells, the SILAC ratios of H4K16ac peptide decreased in respect to

control cells, while di-, tri- and tetra-acetylated forms did not change significantly; the di-acetylated K16ac/K12ac form decreases only in MDA-MB231 cells. Unexpectedly, MCF7 cells displayed an opposite trend, with up-regulation of H4K16ac and H4K16ac/K12ac, paralleled by a decrease of the hyper-acetylated states, more pronounced than in the other cells. We confirmed these observations by Western Blot analysis monitoring H4K5ac, typically used to mark hyper-acetylated H4 N-tails (Fig. 4).

We profiled the levels of class I histone deacetylates (HDAC) in our cell lines, with the aim of investigating the correlation between altered acetylation patterns in H3 and H4 and the enzymes responsible of removing acetyl-groups from histones: HDAC1 and HDAC2 were in general more abundant in breast cancer cell lines than in normal breast epithelial cells. HDAC3 presented a more heterogeneous pattern, with over-expression only observed (compared to MCF10A) in MDA-MB453 and T-47D cells (Fig. 4).

Histone H4 is also methylated at Lysine 20. In fact, we detected mono-, di- and tri-methylation in peptide (20–35) of H4 (Fig. S2). As expected from previous studies, we observed a significant decrease of K20me3 in all breast cancer cells (Fig. 3) (Fraga et al. 2005). Remarkably, we also observed the up-regulation of K20me1, which has not previously been described (Fig. 3).

Discussion

High-resolution MS has already proved powerful in mapping complex hPTMs patterns, overcoming the limitation faced with antibodies, and improving the resolution of nearly isobaric modifications, such as acetylation and trimethylation, on the histone N-terminal tails (Jung et al. 2010). Here we used MS in combination with SILAC strategy, specifically tailored to quantify modified peptides from histones H3 and H4. The application of SILAC to quantify histone modifications required a few adjustments to the regular protocols of protein labeling and sample processing: for instance we labeled cells with only heavy-arginine (Arg10), rather than following the standard double Lys- and Arg-labeling. In addition, we employed endoproteinase Arg-C to digest in-solution histones, in order to obtain peptides of optimal length for the MS analysis, with at least one label at the C-terminus. The use of trypsin is not advisable for the digestion of histones prior MS, because the peptides produced are too small, and consequently of difficult detection in LC–MS. Moreover, the high frequency of modifications occurring on lysines prevents from complete enzymatic digestion by trypsin. This results in a very complex digestion pattern that hampers the site-specific attribution of PTMs and their relative quantitation in different samples. Instead, the SILAC-MS analytical pipeline undertaken allowed separating histone peptides-pairs along the TIC, profiling them by visual inspection, with a relatively fast and precise quantitation of acetyl- and methyl-containing peptides. We profiled 24 distinct modifications at 14 different sites on histones H3 and H4, which were quantified by H/L ratio of the corresponding peptides. Importantly, this approach is uniquely suited to measure relative abundance of distinct hPTMs from different functional states, information that could not be extrapolated with the same accuracy with antibody-based approaches.

Breast cancer is a heterogeneous disease ranging from pre-malignant hyper-proliferation to locally malignant, invasive and metastatic carcinomas. To reflect this heterogeneity, we compared cancer cell lines associated to different features of human breast carcinoma: MCF7 and T-47D cells are ER-positive and hormone sensitive cells correlating with relatively less aggressive and more benign features of breast cancer; instead MDA-MB231 and MDA-MB453 are highly invasive and metastasizing ER-negative cells. Despite the well-recognized fact that the perturbation of hPTMs in breast epithelial cells, along with global DNA hypo-methylation, is a pivotal event in cancer onset and progression, a mechanistic relationship between the two phenomena is still elusive, because the global profile of breast cancer-specific hPTMs is not thoroughly described.

It is of note that in this work we extended the characterization of the PTMs signature of breast cancer and reveal the complexity of the relationship between hPTMs and tumor features. We found several marks whose levels are significantly altered in cancer, compared to normal epithelial breast cells: H3K4me1, H3K9me2, H3K9me3, H3K27me2, H3K27me3, H4K16ac, H4K20me1 (Fig. 3; Fig. S1). With our strategy we could identify not only changes already described in tumors (loss of histone H3K9me3 and reduction of H4K20me3 and H4K16ac) (Fraga et al. 2005; Tryndyak et al. 2006), but also novel PTMs variations, such as on H3K4me1, H3K9me2, H3K27me2-3 and on H4K20me1.

Tri-methylation of H4K20 was already reported to decrease in malignant breast cancer cell lines, compared to non-tumorigenic breast epithelial cells (Tryndyak et al. 2006), and the same loss was also observed in estradiol-induced mammary carcinogenesis in rat (Kovalchuk et al. 2007). Suv4-20h2 enzyme has been reported to be down-regulated in breast cancer cells (Tryndyak et al. 2006), a result that fits well with the H4K20 methylation patterns observed in this work: in fact, lack of Suv4-20 is expected to cause loss of di- and tri-methylation on Lysine 20, with a corresponding increase in mono-methylation, the substrate of reaction. We extended further this analysis and analyzed by western blot the abundance of Pr-SET7, considered the enzyme responsible of (mono-) methylation of H4K20

(Fig. 4): its down-regulation is slight but detectable in MCF7, MDA-MB231 and MDA-MB453, while T47D cells show a strong up-regulation of this protein in respect to both the other cancer lines and control cells, a change of difficult interpretation. The picture is obviously incomplete, because involvement of other enzymes, still uncharacterized cannot be excluded.

In general, the establishment of methylation patterns on H4K20, H3K27 and especially H3K9 is a complex process involving the activity of several different methyltransferases and demethylases (Cedar and Bergman 2009) To shed light, at least partial, to the molecular mechanism underlying the altered methylation patterns observed in cancer cells, we profiled some of the methyltransferases responsible of adding methyl groups on H3K9 and K27, similarly to the analysis of HDACs. Western blots were carried out for the enzymes Suv39h1 and h2, G9a and SETDB1, responsible of modifying Lysine 9 of H3, although G9a was reported to modify H3K27 as well (Tachibana et al. 2001; Ikegami et al. 2007) (Fig. 4). We observed that Suv39h1 appears overall up-regulated in cancer cell lines in respect to MCF10A (excluding MDA-MB231 cells, where the expression of this enzyme is similar to that in control MCF10A cells); this is in partial disagreement with what has previously been reported (Tryndyak et al. 2006), although the panel of carcinoma cell lines under investigation was to some extent different. More intriguingly, we have noticed an inverse correlation between the expression level of Suv39h1 and G9a: in particular, when Suv39h1 is up, G9a appears down-regulated, with an overall underexpression of the enzyme in three of four cancer cell lines (MCF7, MDA-MB453 and T47D); also in this case MDA-MB231 cells behave differently from the trend. Suv39h2 and SETDB1, instead, did not show significant changes in abundance (Fig. 4). The strong inverse correlation between two enzymes impinging on the same residue is fascinating and it emphasizes the intricate functional network existing among the activities responsible of setting up the histone methylation patterns, both in physiological and disease condition. In addition, we cannot exclude that other enzymes, such as de-methylases removing methyl-groups from this residue, might be also aberrantly expressed in cancer. A focused investigation would allow dissecting the intricate network linking the diverse histone modifying enzymes (HMEs), but it is beyond the scope of this work.

Lysine 16 of H4 is down-regulated in MDA-MB231, MDA-MB453 and T-47D with respect to normal epithelial cells, whereas other residues do not show significant changes. Global loss of K16 acetylation has already been observed by immunohistochemistry in a well characterized histologic series of invasive breast carcinomas (Elsheikh et al. 2009; Suzuki et al. 2009) and was defined a hallmark of human cancer (Fraga et al. 2005). Furthermore, in a context of general H4K16 hypoacetylation in cancer, a spectrum of variation of acetylation level at Lysine 16 is observed in different subsets of tumors, correlating with better or worse prognosis (Elsheikh et al. 2009). Interestingly, this observation fits with our finding that at least one cell line with a more benign biological behavior (MCF7 cells) shows an inverse pattern of K16ac. Although the peculiar acetylation pattern of H4 in MCF7 cells is intriguing, it requires further investigation to dissect a potential role of this PTM as diagnostic or prognostic biomarker of breast cancer. Undoubtedly, the observation that MCF7 epigenetics traits on histone H4 differ significantly from the other breast cancer cells, recommend caution when employing this cell line as a model for breast cancer, at least in an epigenetic perspective.

It is now apparent that the extent of acetylation on histone tails depends on the balance between the enzymatic activities of HDAC and histone acetyltransferase (HAT). We profiled the levels of class I histone deacetylase HDAC1, 2, and 3: HDAC1 and HDAC2 were in general more abundant in breast cancer cell lines than in normal breast epithelial cells, while HDAC3 presented a more heterogeneous pattern (Fig. 4). Interestingly, HDAC1 and HADC2 are believed to regulate most of the observed changes in histone acetylation, mainly on Lysines 5, 8, 12 and 16 of histone H4. Recently, it was shown that HDAC1 and HDAC3 are up-regulated in breast cancers (Feng et al. 2007). Nevertheless, immunohistochemistry of HDAC expression in tumor samples unexpectedly indicates that HDAC1, 2 and 6 decrease with progression from normal to ductal carcinoma in situ, to invasive ductal carcinoma (Suzuki et al. 2009). A possible explanation is that the relative contribution of both HATs and HDACs is altered. A recent paper described that expression of hMOF, a CBP-p300 HAT, is lost in a large subset of primary breast carcinomas (Pfister et al. 2008).

The novelty of our study consists in the identification of new PTMs that are altered in the four tumor cell lines: H3K4me1, H3K9me2, H3K27me2-3 and H4K20me1. Intriguingly, few of these marks such as H3K4me1 and H4K20me1 are enriched in transcribed regions of genes and at DNA regulatory elements, whereas H3K9me2 and H3K27me3 are related to gene silencing (Wang et al. 2008). The significant up-regulation of H3K27me3 might be explained in light of the already reported over-expression in breast cancer cells of EZh2, the methyltransferase specific for this residue (Bracken et al. 2003), an increase that we also confirmed (Fig. 4).

Some well-known modifications were not detected in our analysis: for example H3K9ac or H3K4me3; most likely this was due to the low abundance of these marks in these cell types. Moreover, the peptide (27–40) has a large number of putative species, where K27 and K36 can

co-exist in different modification states (e.g. K27me3/K36me1, K27me1/K36me3, and K27me2/K36me3); the complete compilation of all these species could not be uniquely characterized in our analysis. However, Jensen and co-workers recently showed that new MS instruments, such as LTQ Orbitrap Velos, allow the acquisition of MS/MS spectra in high resolution mode, boosting the capability to resolve near-isobaric modifications coexisting on multiple PTM sites within the same peptide (Jung et al. 2010). Although bottom-up approach is sensitive and specific, it falls short in assessing combinations of PTMs, evaluating their relative stoichiometry and measuring the overall abundance of differently modified intact protein species. Top-down allows determining global combinations of PTMs in intact proteins (Siuti et al. 2006), however, it is limited when it comes to the site-specific attribution of modifications in hyper-modified proteins. Furthermore, it shows a lower dynamic range of detection than bottom-up, a limit that can restrict characterization of complex pattern of low abundant modifications, such as the methylation pattern of K27/H36/K37 in peptide H3(27–40). Based on this, we speculate that a synthetic MS approach, combining peptide-based strategy (bottom-up) with larger peptides or intact proteins analysis (top-down and middle-down) will offer the most comprehensive study of histone heterogeneity, however, at the cost of larger amount of starting material and more laborious sample preparation protocols.

Despite these technical limitations, our analytical strategy based on the combination of FT-MS and SILAC is reliable, comprehensive and sensitive in detecting even mild changes in PTMs abundance, with a higher discriminating potential than antibody-based assays. Thus, it can offer an essential contribution to the understanding of epigenetic phenomena in cancer biology.

Acknowledgments TB work is supported by grants from the Giovanni Armenise-Harvard Foundation Career Development Program, the Association of International Cancer Research (AICR), the Associazione Italiana Ricerca sul Cancro (AIRC) and the Fondazione Cariplo. Work in SMi lab is supported by EEC (Epitron) and AIRC. We would like to thank Pietro Spinelli for technical support in cell culture and David Cairns for critical reading of the manuscript.

References

Beck HC (2010) Mass spectrometry in epigenetic research. Methods Mol Biol 593:263–282

Bracken AP, Pasini D, Capra M, Prosperini E, Colli E, Helin K (2003) EZH2 is downstream of the pRB-E2F pathway, essential for proliferation and amplified in cancer. EMBO J 22(20):5323–5335

Burlingame AL, Zhang X, Chalkley RJ (2005) Mass spectrometric analysis of histone posttranslational modifications. Methods 36(4):383–394

Cedar H, Bergman Y (2009) Linking DNA methylation and histone modification: patterns and paradigms. Nat Rev Genet 10(5):295–304

Cosgrove MS (2007) Histone proteomics and the epigenetic regulation of nucleosome mobility. Exp Rev Proteomics 4(4):465–478

Cox J, Mann M (2008) MaxQuant enables high peptide identification rates, individualized p.p.b.-range mass accuracies and proteome-wide protein quantification. Nat Biotechnol 26(12):1367–1372

Dobosy JR, Selker EU (2001) Emerging connections between DNA methylation and histone acetylation. Cell Mol Life Sci 58(5–6):721–727

Elsheikh SE, Green AR, Rakha EA, Powe DG, Ahmed RA, Collins HM, Soria D, Garibaldi JM, Paish CE, Ammar AA, Grainge MJ, Ball GR, Abdelghany MK, Martinez-Pomares L, Heery DM, Ellis IO (2009) Global histone modifications in breast cancer correlate with tumor phenotypes, prognostic factors, and patient outcome. Cancer Res 69(9):3802–3809

Esteller M (2002) CpG island hypermethylation and tumor suppressor genes: a booming present, a brighter future. Oncogene 21(35):5427–5440

Feinberg AP, Vogelstein B (1983) Hypomethylation distinguishes genes of some human cancers from their normal counterparts. Nature 301(5895):89–92

Feng W, Lu Z, Luo RZ, Zhang X, Seto E, Liao WS, Yu Y (2007) Multiple histone deacetylases repress tumor suppressor gene ARHI in breast cancer. Int J Cancer 120(8):1664–1668

Fraga MF, Ballestar E, Villar-Garea A, Boix-Chornet M, Espada J, Schotta G, Bonaldi T, Haydon C, Ropero S, Petrie K, Iyer NG, Perez-Rosado A, Calvo E, Lopez JA, Cano A, Calasanz MJ, Colomer D, Piris MA, Ahn N, Imhof A, Caldas C, Jenuwein T, Esteller M (2005) Loss of acetylation at Lys16 and trimethylation at Lys20 of histone H4 is a common hallmark of human cancer. Nat Genet 37(4):391–400

Freitas MA, Sklenar AR, Parthun MR (2004) Application of mass spectrometry to the identification and quantification of histone post-translational modifications. J Cell Biochem 92(4):691–700

Garcia BA, Shabanowitz J, Hunt DF (2007) Characterization of histones and their post-translational modifications by mass spectrometry. Curr Opin Chem Biol 11(1):66–73

Herman JG, Baylin SB (2003) Gene silencing in cancer in association with promoter hypermethylation. N Engl J Med 349(21):2042–2054

Ikegami K, Iwatani M, Suzuki M, Tachibana M, Shinkai Y, Tanaka S, Greally JM, Yagi S, Hattori N, Shiota K (2007) Genome-wide and locus-specific DNA hypomethylation in G9a deficient mouse embryonic stem cells. Genes Cells 12(1):1–11

Jenuwein T, Allis CD (2001) Translating the histone code. Science 293(5532):1074–1080

Jung HR, Pasini D, Helin K, Jensen ON (2010) Quantitative mass spectrometry of histones H3.2 and H3.3 in Suz12-deficient mouse embryonic stem cells reveals distinct, dynamic post-translational modifications at Lys-27 and Lys-36. Mol Cell Proteomics 9(5):838–850

Kall L, Storey JD, MacCoss MJ, Noble WS (2008) Assigning significance to peptides identified by tandem mass spectrometry using decoy databases. J Proteome Res 7(1):29–34

Kelleher NL, Zubarev RA, Bush K, Furie B, Furie BC, McLafferty FW, Walsh CT (1999) Localization of labile posttranslational modifications by electron capture dissociation: the case of gamma-carboxyglutamic acid. Anal Chem 71(19):4250–4253

Kouzarides T (2007) Chromatin modifications and their function. Cell 128(4):693–705

Kovalchuk O, Tryndyak VP, Montgomery B, Boyko A, Kutanzi K, Zemp F, Warbritton AR, Latendresse JR, Kovalchuk I, Beland FA, Pogribny IP (2007) Estrogen-induced rat breast carcinogenesis is characterized by alterations in DNA methylation, histone

modifications and aberrant microRNA expression. Cell Cycle 6(16):2010–2018

Loyola A, Bonaldi T, Roche D, Imhof A, Almouzni G (2006) PTMs on H3 variants before chromatin assembly potentiate their final epigenetic state. Mol Cell 24(2):309–316

Mann M (2006) Functional and quantitative proteomics using SILAC. Nat Rev Mol Cell Biol 7(12):952–958

Medzihradszky KF, Zhang X, Chalkley RJ, Guan S, McFarland MA, Chalmers MJ, Marshall AG, Diaz RL, Allis CD, Burlingame AL (2004) Characterization of Tetrahymena histone H2B variants and posttranslational populations by electron capture dissociation (ECD) Fourier transform ion cyclotron mass spectrometry (FT-ICR MS). Mol Cell Proteomics 3(9):872–886

Olsen JV, de Godoy LM, Li G, Macek B, Mortensen P, Pesch R, Makarov A, Lange O, Horning S, Mann M (2005) Parts per million mass accuracy on an Orbitrap mass spectrometer via lock mass injection into a C-trap. Mol Cell Proteomics 4(12):2010–2021

Ong SE, Mittler G, Mann M (2004) Identifying and quantifying in vivo methylation sites by heavy methyl SILAC. Nat Methods 1(2):119–126

Pesavento JJ, Kim YB, Taylor GK, Kelleher NL (2004) Shotgun annotation of histone modifications: a new approach for streamlined characterization of proteins by top down mass spectrometry. J Am Chem Soc 126(11):3386–3387

Pfister S, Rea S, Taipale M, Mendrzyk F, Straub B, Ittrich C, Thuerigen O, Sinn HP, Akhtar A, Lichter P (2008) The histone acetyltransferase hMOF is frequently downregulated in primary breast carcinoma and medulloblastoma and constitutes a biomarker for clinical outcome in medulloblastoma. Int J Cancer 122(6):1207–1213

Pokholok DK, Harbison CT, Levine S, Cole M, Hannett NM, Lee TI, Bell GW, Walker K, Rolfe PA, Herbolsheimer E, Zeitlinger J, Lewitter F, Gifford DK, Young RA (2005) Genome-wide map of nucleosome acetylation and methylation in yeast. Cell 122(4):517–527

Rappsilber J, Mann M, Ishihama Y (2007) Protocol for micro-purification, enrichment, pre-fractionation and storage of peptides for proteomics using StageTips. Nat Protoc 2(8):1896–1906

Roth MJ, Forbes AJ, Boyne MT II, Kim YB, Robinson DE, Kelleher NL (2005) Precise and parallel characterization of coding polymorphisms, alternative splicing, and modifications in human proteins by mass spectrometry. Mol Cell Proteomics 4(7):1002–1008

Seligson DB, Horvath S, Shi T, Yu H, Tze S, Grunstein M, Kurdistani SK (2005) Global histone modification patterns predict risk of prostate cancer recurrence. Nature 435(7046):1262–1266

Siuti N, Roth MJ, Mizzen CA, Kelleher NL, Pesavento JJ (2006) Gene-specific characterization of human histone H2B by electron capture dissociation. J Proteome Res 5(2):233–239

Su X, Ren C, Freitas MA (2007) Mass spectrometry-based strategies for characterization of histones and their post-translational modifications. Exp Rev Proteomics 4(2):211–225

Suzuki J, Chen YY, Scott GK, Devries S, Chin K, Benz CC, Waldman FM, Hwang ES (2009) Protein acetylation and histone deacetylase expression associated with malignant breast cancer progression. Clin Cancer Res 15(9):3163–3171

Tachibana M, Sugimoto K, Fukushima T, Shinkai Y (2001) Set domain-containing protein, G9a, is a novel lysine-preferring mammalian histone methyltransferase with hyperactivity and specific selectivity to lysines 9 and 27 of histone H3. J Biol Chem 276(27):25309–25317

Taverna SD, Ueberheide BM, Liu Y, Tackett AJ, Diaz RL, Shabanowitz J, Chait BT, Hunt DF, Allis CD (2007) Long-distance combinatorial linkage between methylation and acetylation on histone H3 N termini. Proc Natl Acad Sci USA 104(7):2086–2091

Thomas CE, Kelleher NL, Mizzen CA (2006) Mass spectrometric characterization of human histone H3: a bird's eye view. J Proteome Res 5(2):240–247

Thorne AW, Kmiciek D, Mitchelson K, Sautiere P, Crane-Robinson C (1990) Patterns of histone acetylation. Eur J Biochem 193(3):701–713

Tryndyak VP, Kovalchuk O, Pogribny IP (2006) Loss of DNA methylation and histone H4 lysine 20 trimethylation in human breast cancer cells is associated with aberrant expression of DNA methyltransferase 1, Suv4–20h2 histone methyltransferase and methyl-binding proteins. Cancer Biol Ther 5(1):65–70

Wang Z, Zang C, Rosenfeld JA, Schones DE, Barski A, Cuddapah S, Cui K, Roh TY, Peng W, Zhang MQ, Zhao K (2008) Combinatorial patterns of histone acetylations and methylations in the human genome. Nat Genet 40(7):897–903

Zhang K, Williams KE, Huang L, Yau P, Siino JS, Bradbury EM, Jones PR, Minch MJ, Burlingame AL (2002) Histone acetylation and deacetylation: identification of acetylation and methylation sites of HeLa histone H4 by mass spectrometry. Mol Cell Proteomics 1(7):500–508